Lateral distributions of EAS muons (E$_\mu$ >800 MeV) measured with the KASCADE-Grande Muon Tracking Detector in the primary energy range 10^{16} eV – 10^{17} eV

W.D. Apel[a], J.C. Arteaga-Velázquez[b], K. Bekk[a], M. Bertaina[c], J. Blümer[a,d], H. Bozdog[a], I.M. Brancus[e], E. Cantoni[c,f,1], A. Chiavassa[c], F. Cossavella[f,2], K. Daumiller[a], V. de Souza[g], F. Di Pierro[c], P. Doll[a], R. Engel[a], J. Engler[a], B. Fuchs[f], D. Fuhrmann[h,3], A. Gherghel-Lascu[e], H.J. Gils[a], R. Glasstetter[h], C. Grupen[i], A. Haungs[a], D. Heck[a], J.R. Hörandel[j], D. Huber[d], T. Huege[a], K.-H. Kampert[h], D. Kang[d], H.O. Klages[a], K. Link[d], P. Łuczak[k,*], H.J. Mathes[a], H.J. Mayer[a], J. Milke[a], B. Mitrica[e], C. Morello[f], J. Oehlschläger[a], S. Ostapchenko[a,4], N. Palmieri[d], M. Petcu[e], T. Pierog[a], H. Rebel[a], M. Roth[a], H. Schieler[a], S. Schoo[a], F.G. Schröder[a], O. Sima[l], G. Toma[e], G.C. Trinchero[c], H. Ulrich[a], A. Weindl[a], J. Wochele[a], J. Zabierowski[k,*]

[a]Institut für Kernphysik, KIT - Karlsruher Institut für Technologie, Germany
[b]Universidad Michoacana, Instituto de Física y Matemáticas, Morelia, Mexico
[c]Dipartimento di Fisica, Università degli Studi di Torino, Italy
[d]Institut für Experimentelle Kernphysik, KIT - Karlsruher Institut für Technologie, Germany
[e]Horia Hulubei National Institute of Physics and Nuclear Engineering, Bucharest, Romania
[f]Osservatorio Astrofisico di Torino, INAF Torino, Italy
[g]Universidade São Paulo, Instituto de Física de São Carlos, Brasil
[h]Fachbereich Physik, Universität Wuppertal, Germany
[i]Department of Physics, Siegen University, Germany
[j]Deptartment of Astrophysics, Radboud University Nijmegen, The Netherlands
[k]National Centre for Nuclear Research, Department of Astrophysics, Łódź, Poland
[l]Department of Physics, University of Bucharest, Bucharest, Romania

Abstract

The KASCADE-Grande large area (128 m^2) Muon Tracking Detector has been built with the aim to identify muons (E_μ^{thr}=800 MeV) in Extensive Air Showers by track measurements under 18 r.l. shielding. This detector provides high accuracy angular information (approx. 0.3°) for muons up to 700 m distance from the shower core. In this work we present the lateral density distributions of muons in EAS measured with the Muon Tracking Detector of the KASCADE-Grande experiment. The density is calculated by counting muon tracks in a muon-to-shower-axis distance range from 100 m to 600 m from showers with reconstructed energy of 10^{16} eV – 10^{17} eV and zenith angle $\theta < 18°$. In the distance range covered by the experiment, these distributions are well described by functions of Greisen type. They are compared also with the distributions obtained with the KASCADE scintillator array (E_μ^{thr}=230 MeV) and with distributions obtained using simulated showers.

Keywords: cosmic rays, extensive air showers, KASCADE-Grande, Muon Tracking Detector, lateral distributions, muon density

1. Introduction

Investigations of the muonic component in extensive air showers (EAS) is of primary importance for understanding air shower physics. Muons carry nearly undistorted information about their parent particles, pions and kaons. These parent particles are the most numerous products of hadronic interactions responsible for the development of the shower cascade in the atmosphere. This longitudinal development contains the information on the nature (mass) of the primary cosmic ray particle, which is related to astrophysical questions. It also carries information relevant to particle physics on the underlying properties of hadronic interactions in the energy range and the kinematical region only recently being accessed by the forward detectors of the LHC [1]. Therefore, study of the mass composition of cosmic rays and the tests of various hadronic interaction models are in many cases related to the investigation of this longitudinal development of showers.

The most common way used by all EAS experiments with sufficient number of muon detectors is the investigation of lateral distributions of muons, being a transformation of the development of the muonic component onto the horizontal plane of the shower [2, 3]. This is usually measured with arrays of scintillation detectors, where the number of muons in each detector is derived from the energy deposited in the scintillators, using non-trivial procedures based on simulations [4, 5].
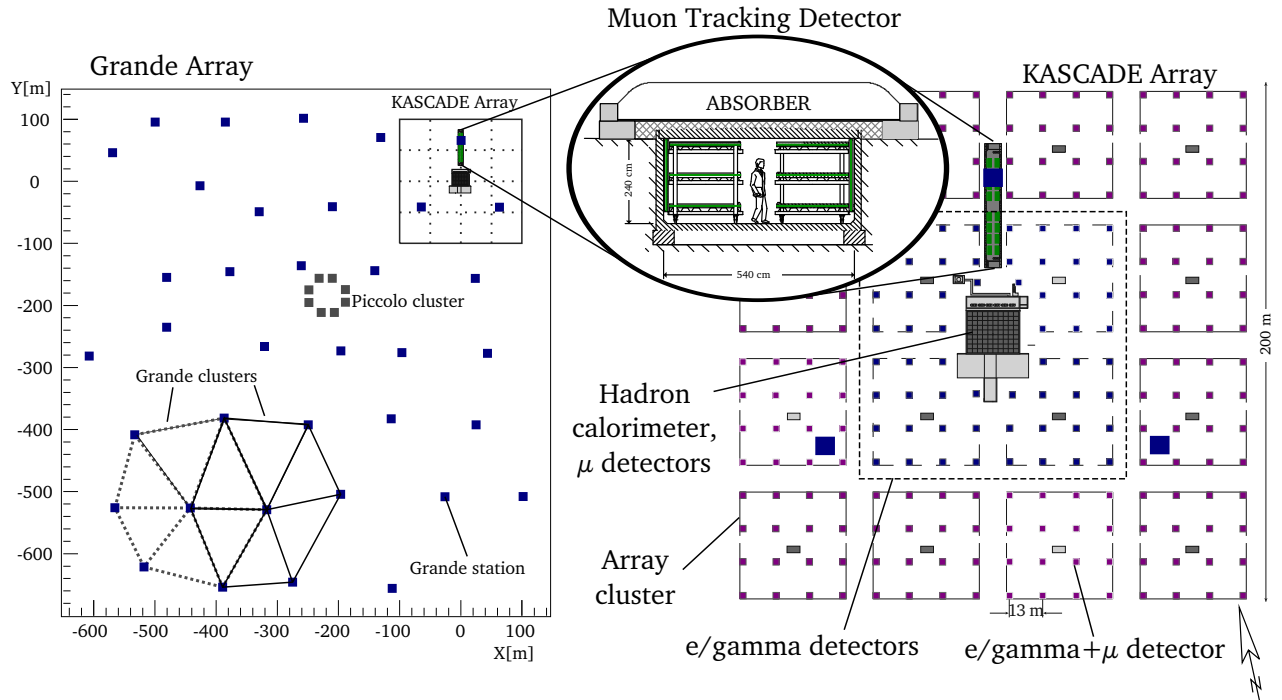
Muon tracking detectors, actually counting muons in EAS,

Figure 1: Layout of the KASCADE-Grande experiment. Note the location of the Muon Tracking Detector (MTD) within the KASCADE Array.

have rather not been used for this purpose due to the difficulty of building sufficiently large detectors of this type. Earlier attempts were based on neon flash tubes, either in tracking [6] or hodoscopic [7] configurations. Muon densities were measured close to the shower core (< 30 m in Ref. [7] and 5 m – 70 m in Ref. [6]), and for shower sizes corresponding to the 'knee' region of the primary energy spectrum, around 10^{15} eV. A possibility of the investigation of muon tracks from more energetic showers at larger distances has been created in the KASCADE-Grande EAS experiment [8], being an extension of the KASCADE experimental setup [9]. It is a multi-detector system (Fig. 1) located on the site of the Karlsruhe Institute of Technology (KIT) – Campus North, Germany at 110 m a.s.l. It was designed to detect the three EAS particle components: hadrons, electrons and muons (at 4 energy thresholds) in a wide range of distances from the shower core (up to 700 m), and for primary particle energies from 5×10^{14} eV to 10^{18} eV. High precision measurements of particle densities and tracks – the latter by means of a dedicated Muon Tracking Detector (MTD) [10] – at different energy thresholds allow to investigate many features of EAS and are the basis for multi-parameter analyses (e.g.: [4, 11]).

In particular, the MTD gives a possibility to study the longitudinal development of EAS. For the first time it was possible to investigate the lateral distribution of muons using the muon tracks in a distance up to several hundred meters from the core from a large number of showers with energies above 10^{16} eV. The results of this investigation are reported in this work.

2. Muon tracking in KASCADE-Grande

The KASCADE-Grande experiment (Fig. 1) contains several detector systems. First, it consists of the KASCADE experimental setup located in the North-East corner, where the MTD is also situated. A detailed description of this part of the experiment and its performance can be found elsewhere [9]. In view of the research presented here, apart from the MTD, an array of 252 detector stations (called the *KASCADE Array*), covering an area of 200 m × 200 m, is an important part of the setup. The stations are placed on a square grid with 13 m spacing and are organized in 16 clusters. Each station is equipped with scintillation counters registering the electromagnetic shower component (E^{thr}=5 MeV), and in the outer 12 clusters, also the muonic part of EAS (E_{μ}^{thr}=230 MeV).

A second major part of KASCADE-Grande is the *Grande Array*, being an extension of the KASCADE Array. It consists of 37 detector stations organized in a hexagonal grid of 18 clusters, covering an area of 0.5 km² [8]. In the centre there is a small trigger array of plastic scintillation stations, called *Piccolo*, built to provide additional fast triggers for some of the KASCADE detector components.

2.1. Design of the MTD

The MTD is located in the northern part of the KASCADE Array (as shown in Fig. 1) and houses 16 muon telescopes made out of *streamer tubes* (ST). The telescopes are placed in a 5.4 × 2.4 × 44 m³ concrete tunnel, additionally buried under an absorber made of iron plates separated with sand. This shielding corresponds to an equivalent of 18 radiation lengths

2

and absorbs most of the low-energetic electromagnetic particles, thus allowing the identification of the tracks from muons with an energy larger than 800 MeV. The streamer tubes in each muon telescope are grouped in four 2×4 m^2 *detector modules*, three horizontal and one vertical (Fig. 1). The horizontal modules are separated by 820 mm. The middle module is located 1.7 m below the level of the KASCADE scintillator array. The total area for detection of vertical muons is 128 m^2.

All telescopes are connected with a gas supply system, high voltage and electronic chain readout system. An extended description of the design, performance and tests of the MTD can be found in Refs. [10], [12] and [13].

When a particle is passing through the modules of the telescope it ionizes the gas in the streamer tubes and charge-streamers are created. As a result a large increase of charge in a small volume of the tube occurs. This charge is inducing a certain charge in the aluminum *strips* above and below the tubes (perpendicular and diagonal, 30° with respect to the *wires* in the ST), respectively (Fig. 2). A coincidence of the signals from wires and strips in each layer is called a *hit*. The tracks are reconstructed out of three or two hits, in three or two modules, respectively.
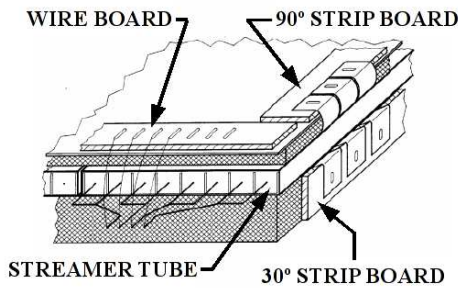

Figure 2: The MTD module design. The PVC boards for fixing signal outputs from wires and strips are shown.

2.1.1. Reconstruction of the muon tracks

From the raw data the information about signals on wires, diagonal and perpendicular strips is retrieved and converted into positions of each wire and strip. The *hit cluster sizes*[5] along the wires and strips (in cm) are reconstructed for each detector module. The position, where the particle crossed the module is estimated as the centre of the cluster and becomes the position of a hit.

Using all hits, the algorithm is searching for hits that can create a track whose direction is correlated with the direction of the shower within an angle of 15°. The 3-hit tracks are reconstructed first. The procedure is then repeated for 2-hit tracks but only for hits that are not involved in 3-hit tracks. The hits that do not fit to any track are ignored.

At muon densities higher than ~0.5 muons/m^2 clusters may

---

[5]Number of wires and strips having signal in each hit used in a track reconstruction is called a hit cluster size.
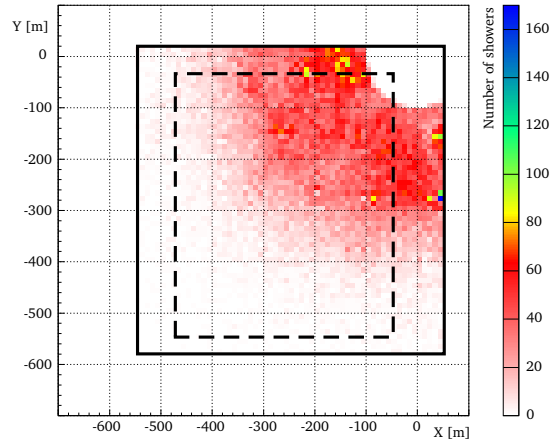

Figure 3: Shower core distribution over the fiducial area used in the MTD analysis (solid-line rectangle). The standard fiducial area (dashed-line rectangle) used in KASCADE-Grande EAS analyses is shown for comparison.

overlap and not all tracks are reconstructed or are reconstructed with poor quality [10]. This reconstruction inefficiency occurs when showers fall too close to the MTD. At extreme cases none of the muon tracks are reconstructed. The minimum distance to the shower core where there is still full reconstruction efficiency increases with shower energy. A more detailed description of the detector response can be found in Refs. [10] and [13].

3. Selection of the data

3.1. Selection of experimental showers

The investigation being a subject of this work is based on more than 45 million showers registered by the KASCADE-Grande experiment from November 2003 to June 2009.

Showers selected for the MTD analysis fulfill general conditions used in the KASCADE-Grande analyses (described in Ref. [8]) and the shower zenith angle is less than 18° to avoid registration problems and the effects of the attenuation of muons originating from more inclined showers. The analysis is done for showers with reconstructed primary energy above 10^{16} eV where KASCADE-Grande provides full detection and reconstruction efficiency for $\theta < 18°$.

The energy of each shower is calculated with the formula:

$$\lg(E_0^{rec}[GeV]) = [a_H + (a_{Fe} - a_H) \cdot k] \cdot \lg(N_{ch}) \quad (1)$$
$$+ \ b_H + (b_{Fe} - b_H) \cdot k$$
$$k = \frac{\lg(N_{ch}/N_\mu) - \lg(N_{ch}/N_\mu)_H}{\lg(N_{ch}/N_\mu)_{Fe} - \lg(N_{ch}/N_\mu)_H} \quad (2)$$

The formula is based on the number of charged particles, obtained with the KASCADE and Grande arrays, and number of muons, obtained with the KASCADE Array muon detectors (see Ref. [14] for details). The energy assignment is defined as E=$f(N_{ch}, k)$, where N_{ch} is the size of the charged particle component and the parameter k is defined through the ratio of the sizes of the charged N_{ch} and muon N_μ components. The
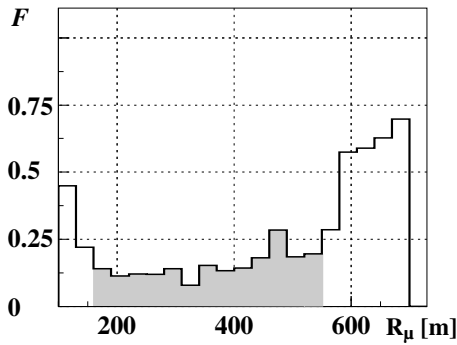
3

Figure 4: Example of the fraction F of showers triggered by KASCADE Array but without reconstructed muon tracks in the primary energy range $\lg(E_0^{rec}[\text{GeV}])=7.6 - 7.9$. Region with constant F (plateau) within one standard deviation is indicated with grey area.

parameters a and b are obtained by Monte Carlo simulations (QGSJet-II-2+FLUKA) and are optimized for the energy and zenith angular range of interest for the present analysis.

The MTD registration is fully efficient in a certain distance range to the shower core. Close to the core the track reconstruction efficiency is affected by the high density of muons that create overlapping hit clusters, and the saturation of the data acquisition system. At larger distances, where the muon density becomes smaller, the registered number of showers with at least one muon is further reduced by trigger and registration inefficiency effects[6] (see Ref. [13]). This leads to the core distribution of showers available for the investigation in the MTD shown in Fig. 3. Most of the showers are located within the standard KASCADE-Grande fiducial area around the centre of the Grande Array (dashed-line rectangle). To enlarge statistics of the number of showers with muons used in the MTD analysis it was necessary to increase this area (solid-line rectangle). This extension, however, has no influence on the quality of reconstructed showers used in the MTD analysis.

The above mentioned inefficiencies result also in showers passing all selection criteria and having KASCADE trigger but not having muons in the MTD (N_{s0}). The fraction of such showers $F = N_{s0}/N_{st}$, where N_{st} is the total number of selected showers, depends on the shower-to-MTD distance and on the primary energy range. An example of the distribution of this fraction for $\lg E_0^{rec}$ interval equal to $7.6 - 7.9$ is shown in Fig. 4. At small distances saturation effects and reconstruction problems dominate while at large distances trigger inefficiencies seem to be more pronounced. In the plateau region F is constant within one standard deviation. Examination of the showers without muons did not show any difference between their characteristics and the characteristics

---

[6] The MTD is triggered by the KASCADE Array. The showers detected far away from the KASCADE centre not always generate a KASCADE trigger. Moreover, in such showers, the delay of the KASCADE trigger signal reaching the MTD may be too large for fully efficient registration of all muons reaching the MTD.

of the showers with muons in the MTD. So, this points to the explanation of the missing muons rather by the experimental reasons than by the physical ones (fluctuations towards lower densities). Moreover, the Poisson probability of not having a muon in the showers on the plateau is of the order $10^{-3} - 10^{-4}$, what further confirms the instrumental origin of not having a muon. Therefore, in the plateau region of the F distribution we treat such cases in a similar way like those when the MTD was not operating and for the following analyses only showers N_s, with muon tracks, are taken into account.

3.2. Selection of muons

The standard set of parameters used in the description of muon directions obtained with the MTD contains:
a) coordinates of the point where the muon track crosses the plane of the KASCADE scintillator array, b) azimuth and zenith angles of the track, c) hit cluster size, d) the track pattern describing which modules were involved in the track reconstruction.

Due to the reconstruction inefficiency effects it was necessary to restrict the muon-to-shower-axis distance (R_μ), calculated from the shower core position obtained with the Grande Array and the track position in the shower coordinate system, to be larger than 100 meters.

3.3. Analysis of the simulated data

In the standard KASCADE-Grande simulation set, EAS were simulated with CORSIKA [15] using QGSJet-II-2 [16] as a high-energy and FLUKA2002.4 [17] as a low-energy interaction models. Showers were simulated for H, He, C, Si and Fe primaries with an energy spectrum E^{-2} in the energy range from 10^{14} eV to 10^{18} eV and in the zenith angle range $0° - 42°$.

In the standard simulation set, due to the location of the MTD within the experiment and the relatively small detection area, as well as the higher muon energy threshold, the number of simulated events with muon tracks was too small for statistically significant comparisons with the experimental data. To overcome this problem and to lessen the bias in parameter values created by multiple use of CORSIKA simulated showers a special set of proton and iron initiated showers was generated with a QGSJetII+FLUKA model combination. Showers were simulated only up to 20° in zenith angle and each shower was in the detector simulations used 5 times only over the fiducial area used in the MTD analysis.

In the following analysis, the selection of simulated showers and muons is identical to the one for the experimental data, and the shower energy assignment is done with the reconstructed parameters. In addition, all simulated showers fulfill the *software trigger* condition that at least 10 stations in one of the outer clusters of the KASCADE Array have a signal from e/γ detectors above the threshold. This condition is an equivalent of the experimental condition that the MTD is being triggered by the KASCADE Array.
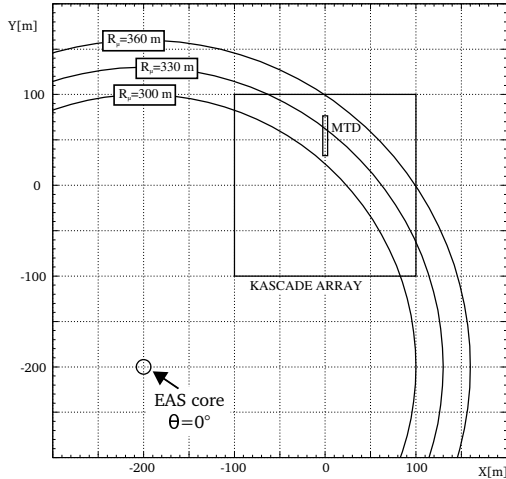
Figure 5: Distance between the muon track and the shower axis R_μ is divided into 30-meter bins. In each bin the number of muon tracks and the area of the MTD are calculated.

4. Lateral muon density distributions

4.1. Description of the analysis

The geometry of a typical shower event is shown in Fig. 5. The vertical shower hits the ground in the Grande Array. The core position, direction and other parameters are reconstructed with the information from the arrays of charged particles and muon detectors.

To obtain the lateral distributions of muons registered in the MTD the following procedure was applied:

1. For each shower, the distance R_μ was divided into 30-meter-wide radial bins around the reconstructed shower core position in shower coordinates.

2. In each distance bin, the number of muons was calculated using the position of the hit in the middle detector module in 3-hit tracks or extrapolation of the position of the hit to the level of the middle detector module in 2-hit tracks for each reconstructed track.

3. The calculation of the area of the detector in each distance bin is done in the following way. In a standard set of data taking two neighbouring wires are combined. With the perpendicular strip they create a 20×20 mm^2 cell that is a basic detection area in the module. With the positions of wires and strips, the location of each cell is calculated and its size added to the detector area contained in the particular R_μ bin. The area was corrected for the zenith angle of a shower multiplying it by the cosine of this angle.

The number of reconstructed muon tracks may be distorted by the data acquisition and/or trigger inefficiencies [13]. As a result, one can obtain no tracks in a distance bin even if the size of the detector area, and the registered muon density in the neighbouring bin make such a zero-track registration highly improbable. Therefore, it was necessary to impose an additional condition to calculate the area in each distance bin. For the muon density calculations only the area in distance bins where at least one muon track was reconstructed was taken into account. Such an approach is equivalent to the case of having a different active detector area for each shower. Without this condition the detector area without muons would be accumulated and the calculated density of muons could be strongly biased towards lower values, especially at distances where the above mentioned inefficiencies have significant influence on the results. As it will be shown below, for every investigated primary energy there exists a shower-to-muon distance range where these inefficiencies have no or negligible effect.

For most of the showers the MTD was divided in two distance bins (78% of the showers) or was fully contained in one distance bin only (12% of the showers). If the two parts were of similar size the muons were usually detected in both of them. In the rest 10% of the showers when the MTD was divided into three parts (three distance bins), in all cases the middle part always had muons, and one of the others, small ones, could have been rejected if there were no muons in it.

The rejection of one part of the detector area could occur in one of the two cases: when the saturation of the data acquisition took place and/or when the two parts differed significantly in size. In the latter case the probability to observe a muon in the rejected ($< 10\% - 20\%$ of the full area) part of the detector was very small but non-zero one. Therefore, a systematical bias towards higher density values may have been introduced. In the analysis this bias was minimized and its final value was estimated.

The density in each distance bin was calculated as a sum of all muons from all showers, corrected for reconstruction efficiency, being divided by the detector area in that distance bin, corrected for zenith angle (A_{MTD}).

$$\rho_i = \frac{\sum_{k=1}^{N_s} (N_{tr2}^{k,i} + N_{tr3}^{k,i}) \cdot \mathcal{K}}{\sum_{k=1}^{N_s} A_{MTD}^{k,i}} \tag{3}$$

where i is the distance bin number, N_s is the number of showers, $A_{MTD}^{k,i}$ is the detector area in i^{th} distance bin for the kth shower, and $\mathcal{K}$ is a track reconstruction efficiency correction factor [13].

4.2. Determination of the MTD full-efficiency distance ranges

The lateral muon density distributions in EAS obtained with muon tracks were investigated in the primary CR energy range from 10^{16} eV to 1.6×10^{17} eV (in four energy sub-ranges, energy calculated with formula (1)) in the muon-to-shower-axis distance from 100 m to 700 m.

Historically, the parametrization of the measured lateral distributions was usually done with Greisen [18], NKG [19] or Lagutin [20] type lateral distribution functions (LDF). These functions describe the lateral density distributions differently in the distance range close to and far away from the shower core. The first two describe equally well the measured distributions of muon densities at different energy thresholds up to 200 m [4], the Lagutin function was applied to describe the lateral distributions in distance range 100 m – 600 m [8].

The functional relation will only describe well the measurement in the muon-to-shower-axis distance where the above
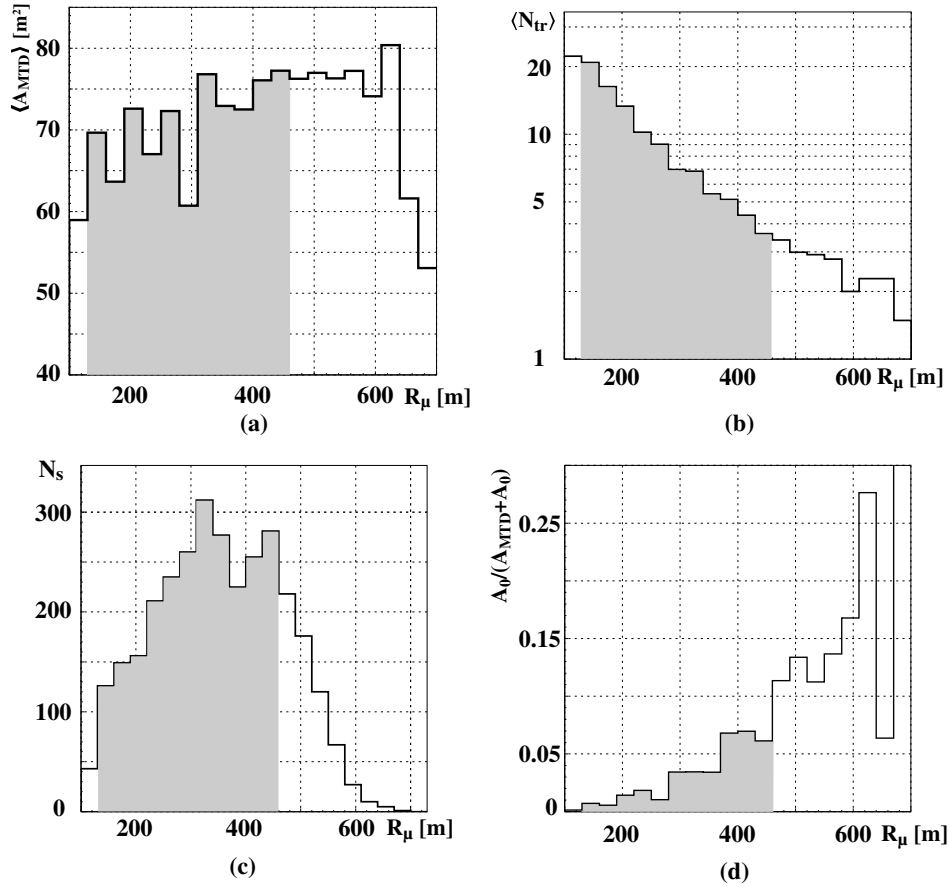
5

Figure 6: Lateral distributions of the following quantities for the primary energy range $\lg(E_0^{rec}[\text{GeV}])=7.3 - 7.6$: (a)$\langle A_{MTD} \rangle$, (b) $\langle N_{tr} \rangle$, (c) the number of showers N_s and (d) the ratio of the empty detector area A_0 to the sum $A_{MTD} + A_0$. Full-efficiency distance range (FR) is marked with grey area.

mentioned inefficiencies have negligible effect. Therefore, prior to the application of any fitting procedure the MTD *full-efficiency distance ranges* (FR) were determined for each of the four primary energy intervals, in $\lg(E_0^{rec}[\text{GeV}])$ equal to: $7.0 - 7.3$, $7.3 - 7.6$, $7.6 - 7.9$ and $7.9 - 8.2$. In these ranges the efficiency has its maximum and is constant in value.

In each FR all of the following conditions should be fulfilled:

1. The number of showers N_s passing the shower and muon selection criteria in all 30-meter distance bins is not smaller than the mean value by more than two standard deviations[7];

2. The value of the detector area with muons A_{MTD} does not differ from the mean detector area with muons $\langle A_{MTD} \rangle$ by more than one standard deviation.

3. The mean number of muon tracks $\langle N_{tr} \rangle$ registered in the far end of the full efficiency distance range is larger than three.

4. The fraction F of showers without muons in the MTD in the whole number of KASCADE-triggered showers should have minimum value being constant within one standard deviation.

The third condition is introduced in order to minimize the systematic error due to the rejection of detector areas without muon tracks (called *empty detector areas*).

The forth condition allows not to consider showers without muons in the analysis.

In Fig. 6, as an example, for the primary energy range $\lg(E_0^{rec}[\text{GeV}])=7.3 - 7.6$ the lateral distributions of the following quantities are shown: the mean detector area with muons $\langle A_{MTD} \rangle$ (a), the mean number of muon tracks $\langle N_{tr} \rangle$ (b), the number of showers N_s (c), and the ratio of the empty detector area A_0, not considered in density calculations, to the sum $A_{MTD}+A_0$ (d), being a measure of the systematic error of the method.

As seen in Fig. 6(d) the accumulated empty detector area increases with the distance, reaching at the far-end distance bin of the FR approx. 10%. Therefore, calculation of the muon density including this area would result in lower values by maximum of this amount. The statistical errors of the muon densities (being shown in figures $7 - 9$) also do not exceed this

---

[7]In the two highest energy intervals – one standard deviation only.
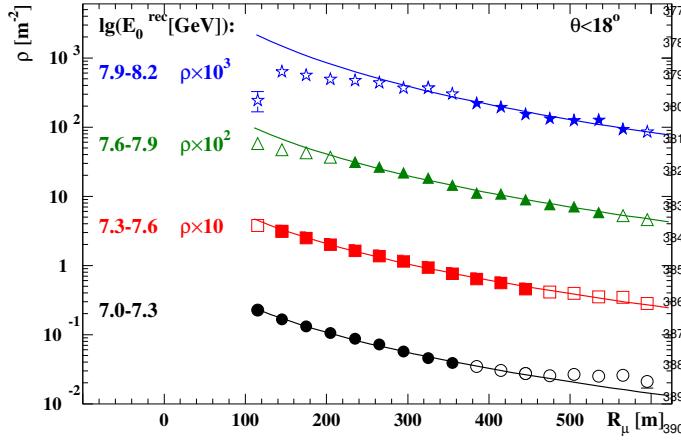
6

Figure 7: Lateral density distributions of muons from the MTD in four primary energy ranges. The distributions can be described by the Greisen function in the distance ranges (FR) marked with full symbols. Only statistical errors are shown.

value. In Table 1 the results of the determination of the MTD full-efficiency distance ranges are summarized.

4.3. Results and discussion

The lateral muon density distributions in EAS obtained with muon tracks are presented in Fig. 7.

In all energy intervals the lateral distributions obtained with the MTD are fitted with a function proposed by Greisen for the muonic component (E_μ^{thr}=1 GeV)[8] :

$$\rho(r) = C \left(\frac{r}{r_G} \right)^{-0.75} \left(1 + \frac{r}{r_G} \right)^{-2.5} \quad (4)$$

where $C = \text{const.} \cdot N_\mu$, r_G is the Greisen radius. In this analysis the fitted parameters are r_G and the scaling factor C of the distributions.

The values of the C and r_G fit parameters are presented in Table 2. The distributions were fitted in the MTD full efficiency ranges, as determined above. In Fig. 7 the experimental MTD-points used in the fits are marked with full symbols.

It is worth to note that the LDFs become steeper with the

---

[8]It is also well suited for our analysis because only less than 5% of muons above 800 MeV have energy below 1 GeV. Moreover, our effective threshold is slightly higher because muons are mostly not vertical ($\langle\theta\rangle \approx 13.3° \pm 0.2°$)

energy of the EAS (the value of r_G is decreasing). This is due to the fact that with increasing energy the shower penetrates deeper into the atmosphere. The same behaviour was observed for muon and electron LDFs in the KASCADE Array [4].

It has been observed, especially seen in the 3rd and 4th energy range, that the LDFs for the KASCADE Array (E_μ^{thr}=230 MeV) are flatter than the LDFs for the MTD muons (E_μ^{thr}=800 MeV) confirming the known dependence of the r_G value in Greisen's formula on the muon energy threshold. This is related to the decrease of the muon parent production angle ($\theta_\pi \simeq p_t/E$) with muon energy and to the weaker multiple Coulomb scattering ($\theta_s \propto 1/E_\mu$).

The shape of the lateral muon density distributions in those distances selected for the Greisen fits allows one to fit them equally well also with a Lagutin-type function.

For instance, in the first energy bin, the MTD distribution has been fitted with the Greisen function in the distance range from 100 m to 370 m, however the experimental points are well on the fitting line up to 460 m. At that distance the F value exceeds 0.6 but the remaining registered 384 showers with muons in the MTD provide enough statistics to obtain this agreement. At larger distances the MTD distribution is rising, as well as the uncertainty of the density values due to decreasing number of showers and muons there. In the last energy bin, the MTD distribution was fitted with the Greisen function in the distance range from 370 m to 580 m. In distances outside this range the MTD distribution gives lower (<370 m) or higher (>580 m) values than predicted by the Greisen function, and the uncertainties of the densities are increasing.

Outside the MTD full-efficiency distance ranges the deviations of the experimental points from the Greisen type functional dependence are seen due to the various inefficiencies discussed above. They are responsible for the shape of the MTD muon lateral density distributions at large distances changing the population of showers with muon tracks reconstructed with the MTD in that distance range.

4.4. Comparison with lateral density distributions from simulations and KASCADE Array

For the purpose of testing the interaction models used in the EAS simulations the comparisons of the experimental muon density distributions at two energy thresholds, obtained with the MTD and with the KASCADE Array, with simulated

Table 1: MTD full-efficiency distance ranges (FR) in four primary energy intervals.

lg(E_0^{rec}[GeV])	FR [m]	$\langle N_s \rangle$	$\langle A_{MTD} \rangle$[m²]
7.0 − 7.3	100 − 370	782±256	72±3
7.3 − 7.6	130 − 460	226±57	71±5
7.6 − 7.9	220 − 550	68±12	72±6
7.9 − 8.2	370 − 580	22±3	69±8

Table 2: Fit parameters C and r_G of the lateral density distributions of muons obtained with the MTD.

lg(E_0^{rec}[GeV])	C[m⁻²]	r_G[m]	χ^2/NDF
7.0 − 7.3	0.151±0.006	441±10	19/7
7.3 − 7.6	0.30±0.02	434±14	14/9
7.6 − 7.9	1.0±0.1	325±15	5/9
7.9 − 8.2	3.4±0.6	247±19	4/5
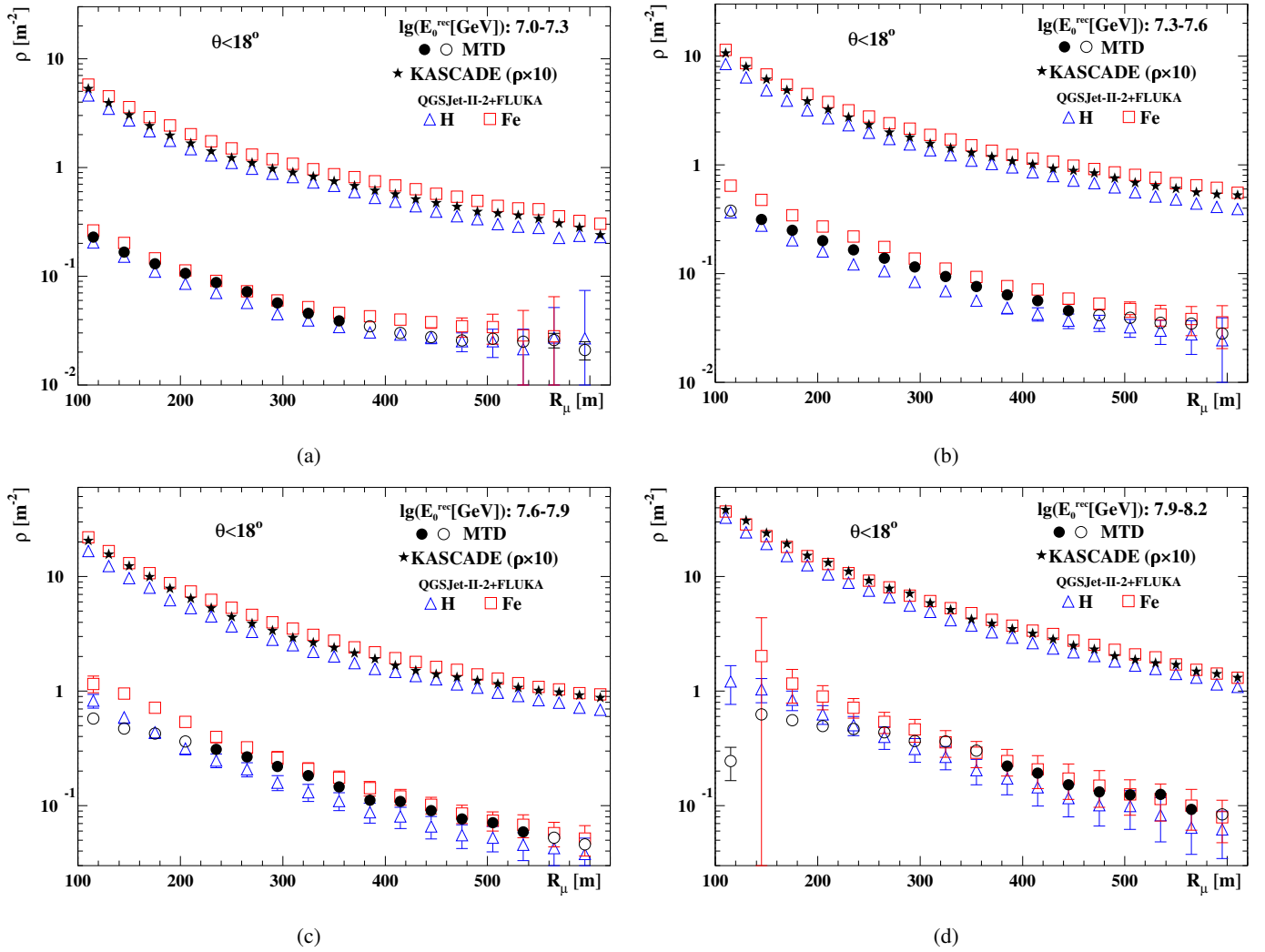
Figure 8: Lateral muon density distributions obtained with the MTD ($\bullet$, $\circ$) and KASCADE Array measurements ($\star$) together with CORSIKA simulations ($\triangle$, $\square$) in the primary energy ranges: (a) $\lg(E_0^{rec}[\text{GeV}])=7.0-7.3$, (b) $\lg(E_0^{rec}[\text{GeV}])=7.3-7.6$, (c) $\lg(E_0^{rec}[\text{GeV}])=7.6-7.9$, (d) $\lg(E_0^{rec}[\text{GeV}])=7.9-8.2$. The lateral distributions obtained with the KASCADE Array are multiplied by factor 10. Only statistical errors are shown.

ones have been done. Simulations were performed for H and Fe primary initiated showers using CORSIKA with QGSJet-II-2+FLUKA2002.4 hadronic interaction models. The results are shown in Fig. 8.

In all energy bins the presented simulations reproduce the experimental distributions within error bars in the sense that the experimental data is bracketed by the simulations with proton and iron primaries, i.e. no unexpected physical processes are visible. However, in case of the MTD distributions, in the distance range up to 200 m (clearly visible in the 3rd and 4th energy bin) the densities for simulations are higher than the densities for the measurement. This is due to the idealized description of the MTD in the detector simulation code that "fails" in reproducing the detector behaviour in extreme cases of high muon density events, when the saturation of the data acquisition and overlapping hit clusters occur.

Further tests of hadronic interaction models can be done

by calculating the ratios of the muon densities obtained for different threshold energies. By investigating such a ratio a sensitivity to the muon energy spectrum in high-energy air showers could be achieved. However, due to the small differences in the muon densities between proton and iron initiated showers, as well as the experimental uncertainties it is difficult to extract a parameter which is both, sensitive to composition and the validity of the hadronic interaction model.

In earlier analyses of the $R_{\rho_1/\rho_2}=f(\lg E)$ dependence described in Refs. [21, 22, 23], the muon density ratios for different energy thresholds measured in KASCADE were investigated (e.g. $R_{2.4/0.49}=\rho_{2.4}/\rho_{0.49}$, $R_{0.49/0.23}=\rho_{0.49}/\rho_{0.23}$). Those investigations were done in the energy range $\lg(E_0^{rec}[\text{GeV}])=6.0-7.0$ and in the distance from 30 m to 70 m. Comparison of several hadronic interaction model combinations (e.g. QGSJet1998+GHEISHA) with the data revealed significant differences between the distributions of
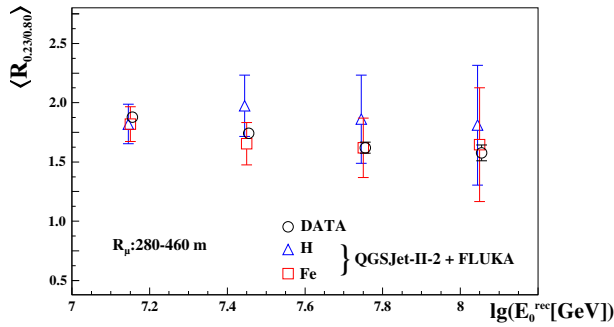
Figure 9: Mean muon density ratio for data and simulations at the distance from 280 m to 460 m at two energy thresholds as a function of the shower energy. The points are shifted for better visibility. Only statistical errors are shown.

the density ratios. The conclusion was that the simulations could not describe well the measurements, but a more detailed quantification was hampered by experimental and methodical uncertainties.

In this analysis we investigate $R_{0.23/0.8}$, the ratio of $\rho_{0.23}$ and $\rho_{0.8}$ which are the densities of muons with energy above 0.23 GeV from the KASCADE and 0.8 GeV from the MTD, and its dependence on shower energy $R_{0.23/0.8}=f(\lg(E_0^{rec}))$.

In Fig. 9 the dependence of the mean muon density ratio calculated with the mean densities in R_μ distance from 280 m to 460 m (see Figure 7) in four energy intervals is shown.

The decrease of the mean density ratio for data is of the order of 10% per decade of the shower energy, however with large statistical errors. A similar decrease can be observed in the simulations where the ratios for iron showers follow the ratios from the measurement. This behaviour shows the trend similar to other investigations of the mass composition at KASCADE-Grande, which indicate that at these energies the composition is significantly heavier than proton.

The presented $R_{0.23/0.8}$ analysis indicates only that, as in the case of lateral muon distributions, the description of the experimental data by the simulations with QGSJet-II-2+FLUKA2002.4 model combination does not require inclusion of any exotic processes. A more detailed quantification, similarly as in the previous density ratio investigations in KASCADE, is impossible due to the experimental uncertainties.

5. Summary and conclusions

Employing the large and precise muon tracking device in KASCADE-Grande the use of the tracking technique for the muon lateral distribution measurements has been revived. For the first time the lateral density distributions of EAS muons (E_μ^{thr}=800 MeV) have been obtained by counting muon tracks for radial distance 100 m – 600 m, in four primary energy ranges above 10^{16} eV and with high statistical accuracy.

The obtained results validate the excellent performance of the MTD, which has already delivered valuable results on the muon production heights, cosmic ray composition and model

tests [24, 25, 26].

The MTD distributions can be described with the Greisen function, however in a limited distance range, different for each energy interval. This is due to the limited efficiency of track reconstruction in the MTD, caused by the saturation of the detector, as well as by trigger inefficiency.

The LDFs from the MTD become steeper with the energy of the showers. The same behaviour was observed for the muon and electron LDFs obtained with the KASCADE Array, as shown in Ref [4]. The dependence of the shape of lateral muon distribution (r_G value in Greisen's formula) on muon threshold energy was observed.

The lateral distributions obtained with the MTD are compared with the density distributions based on energy deposits obtained with the KASCADE Array of scintillator detectors (E_μ^{thr}=230 MeV) for the same sample of EAS. The measured distributions are compared with distributions in simulated showers, QGSJet-II-2+FLUKA2002.4 model combination, Hydrogen and Iron initiated EAS. The comparisons of the lateral muon density distributions, as well as of the density ratio $R_{0.23/0.8}$ show that the MTD and KASCADE results are bracketed by the simulated distributions i.e. no unexpected physical processes are visible. This indicates that the hadronic interaction models have been significantly improved because the simulations performed with earlier models, like QGSJet1998+GHEISHA, could not describe the KASCADE air shower data.

[1] T. Pierog, EPJ Web Conf. 52 (2013) 03001.
[2] L. Pentchev, P. Doll, H. O. Klages, J. Phys. G 25 (1999) 1235.
[3] L. Pentchev, P. Doll, J. Phys. G 27 (2001) 1459.
[4] T. Antoni, et al. (The KASCADE Collaboration), Astropart. Phys. 14 (2001) 245–260.
[5] W. Apel, et al. (KASCADE-Grande Collaboration), Astropart. Phys. 24 (2006) 467 – 483.
[6] F. Ashton, J. Fatemi, H. Nejabat, A. Nasri, W. S. Rada, E. Shaat, A. C. Smith, T. R. Stewart, M. G. Thompson, M. W. Treasure, I. A. Ward, in: Proc. 15th ICRC, 1977, volume 11, Plovdiv, Bulgaria, p. 400.
[7] M. Samorski, W. Stamm, in: Proc. 18th ICRC, 1983, Bangalore, India.
[8] W. D. Apel, et al. (The KASCADE-Grande Collaboration), Nucl. Instrum. Meth. A 620 (2010) 202–216.
[9] T. Antoni, et al. (KASCADE Collaboration), Nucl. Instrum. Meth. A 513 (2003) 490–510.
[10] P. Doll, W. Bartl, C. Büttner, K. Daumiller, K.-H. Kampert, H. Klages, D. Martello, R. Obenland, L. Pentchev, J. Zabierowski, Nucl. Instrum. Meth. A 488 (2002) 517 – 535.
[11] W. Apel, et al., Astropart. Phys. 29 (2008) 412–419.
[12] J. Zabierowski, P. Doll, Nucl. Instrum. Meth. A 484 (2002) 528–532.
[13] P. Łuczak, "Investigation of muons in extensive air showers with the KASCADE-Grande Muon Tracking Detector", Ph.D.

thesis, National Centre for Nuclear Research, Poland, 2012. http://www.ncbj.gov.pl/node/1951.

[14] M. Bertaina, et al. (KASCADE-Grande Collaboration), in: Proc. 31th ICRC, 2009, Lodz, Poland. FZKA 7516, p13-16 (0323).

[15] D. Heck, et al., "CORSIKA: a Monte Carlo code to simulate extensive air showers", Technical Report 6019, Forschungszentrum Karlsruhe(FZKA), 1998.

[16] S. Ostapchenko, Nucl. Phys. B (Proc. Suppl.) 151 (2006) 143–146.

[17] A. Ferrari, P.R. Sala, A. Fasso, and J. Ranft, "FLUKA: a multi-particle transport code", Technical Report, CERN, 2005. CERN-2005-010 ; INFN-TC-2005-11 ; SLAC-R-773.

[18] K. Greisen, Ann. Rev. Nuc. Sci. 10 (1960) 63–108.

[19] K. Kamata, J. Nishimura, Prog. Theor. Phys. Suppl. 6 (1958) 93–155.

[20] A. A. Lagutin, A. V. Pljasheshnikov, V. V. Uchaikin, in: Proc. 16th ICRC, 1979, volume 7, Kyoto, Japan, p. 18.

[21] A. Haungs, et al., Nucl. Phys. B (Proc. Suppl.) 151 (2006) 167 – 174.

[22] A. Haungs, et al. (The KASCADE Collaboration), in: Proc. 28th ICRC, 2003, Tsukuba, Japan. FZKA 6890 p.37-40.

[23] A. Haungs, et al. (The KASCADE-Grande Collaboration), in: Proc. 29th ICRC, 2005, volume 6, Pune, India, pp. 281–284.

[24] W. Apel, et al. (KASCADE-Grande Collaboration), Astropart. Phys. 34 (2011) 476 – 485.

[25] P. Łuczak, et al. (KASCADE-Grande Collaboration), in: Proc. 33rd ICRC, 2013, Rio de Janeiro, Brasil. arXiv:1308.2059.

[26] J. Zabierowski, et al. (KASCADE-Grande Collaboration), in: Proc. 30th ICRC, 2007, volume 4, Merida, Mexico, pp. 111–114.